# Genomic characterization uncovers transmission dynamics of Marburg Virus in Rwanda following a single zoonotic spillover event

**Yvan Butera**[1,2,&,*], **Leon Mutesa**[1,3,4,&,*], Edyth Parker[1,5,6], Raissa Muvunyi[1,7], Esperance Umumararungu[1,7], Alisen Ayitewala[1,4], Jean Pierre Musabyimana[1,7], Alhaji Olono[1,5], Placide Sesonga[1,3,4], Olusola Ogunsanya[1,5], Emmanuel Kabalisa[1,7], Oluwatobi Adedokun[1,5], Nelson Gahima[1,7], Laetitia Irankunda[1,7], Chantal Mutezemariya[1,7], Richard Niyonkuru[1,7], Arlene Uwituze[1,7], Ithiel Uwizera[1,7], James Kagame[1,7], Arlette Umugwaneza[1,7], John Rwabuhihi[1,7], Fidele Umwanankabandi[1,7], Valens Mbonitegeka[1,7], Edouard Ntagwabira[1,7], Etienne Kayigi[1,7], Gerard Izuwayo[1,7], Herve Murenzi[1,7], Therese Mukankwiro[1,7], Nasson Tuyiringire[1,7], Jean Marie Vianney Uwimana[1,7], Agnes Gasengayire[1,7], Reuben Sindayiheba[1,7], Glory-Ugochi Onyeugo[1,4], Merawi Aragaw[1,4], Lenny Gitundu[1,4], Radjabu Bigirimana[1,4], Mosoka Fallah[1,4], Adaora Ejikeme[1,4], Senga Sembuche[1,4], Alice Kabanda[1,4], Jean Claude Mugisha[1,3,4], Emmanuel Edwar Siddig Francis[1,4], Pierre Gashema[1,4], Jerome Ndayisenga[1,4], Alexis Rugamba[1,3], Faustin Kanyabwisha[1,3], Gad Murenzi[1,3], Anise Happi[5], Jean Claude Semuto Ngabonziza[1,7], Misbah Gashegu[1,7], Ayman Ahmed[1,4,7], Noella Bigirimana[1,7], Edson Rwagasore[1,7], Muhammed Semakula[1,2], Jean Paul Rwabihama[1,2,8], Clarisse Musanabaganwa[1,7], Eric Seruyange[1,8,9], Menelas Nkeshimana[1,2], Theogene Twagirumugabe[1,10], David Turatsinze[1,11], Eric Remera[1,7], Noel Gahamanyi[1,7], Sofonias Kifle Tessema[1,4], Isabelle Mukagatare[1,7], Sabin Nsanzimana[1,2], **Christian Happi**[1,5,12,§,*], **Claude Mambo Muvunyi**[1,7,§,*]

[&]*First authors with equal contribution*

[§]*Last authors with equal contribution*

24

25 [1]*Rwanda Joint Task Force for Marburg Virus Disease Outbreak, Ministry of Health, Rwanda*

26 *Biomedical Centre, Kigali, Rwanda*

27 [2]*Ministry of Health, Kigali, Rwanda*

28 [3]*Center for Human Genetics, College of Medicine and Health Sciences, University of Rwanda,*

29 *Kigali, Rwanda*

30 [4]*Africa Centre for Disease Control and Prevention, Addis Ababa, Ethiopia*

31 [5]*African Center of Excellence for Genomics of Infectious Diseases, Redeemer's University, Ede,*

32 *Osun State, Nigeria*

33 [6]*Department of Immunology and Microbiology, The Scripps Research Institute, La Jolla, CA,*

34 *USA*

35 [7]*Rwanda Biomedical Centre, Kigali, Rwanda*

36 [8]*Department of Internal Medicine, College of Medicine and Health Sciences, University of*

37 *Rwanda, Kigali, Rwanda*

38 [9]*Rwanda Military Referral and Teaching Hospital, Kigali, Rwanda*

39 [10]*Butare University Teaching Hospital, Huye, Rwanda*

40 [11]*Kigali University Teaching Hospital, Kigali, Rwanda*

41 [12]*Department of Immunology and Infectious Diseases, Harvard T H Chan School of Public*

42 *Health, Boston, MA 02115, USA*

43

44

45

46 *Corresponding authors

47 Yvan Butera, MD, PhD

48 Ministry of Health

49 Kigali, Rwanda

50 Email: yvan.butera@moh.gov.rw

51

52 Leon Mutesa, MD, PhD

53 Centre for Human Genetics

54 College of Medicine and Health Sciences

55 University of Rwanda

56 Kigali, Rwanda

57 Email: l.mutesa@ur.ac.rw

58

59 Christian Happi, MSc, PhD

60 African Center of Excellence for Genomics of Infectious Diseases,

61 Redeemer's University,

62 Ede, Osun State, Nigeria

63 Email: happic@run.edu.ng

64

65 Claude Mambo Muvunyi, MD, PhD

66 Rwanda Biomedical Centre

67 Kigali, Rwanda

68 Email : claude.muvunyi@rbc.gov.rw

***Abstract***

The ongoing outbreak of Marburg virus disease (MVD) in Rwanda marks the third largest historically, though it has exhibited the lowest fatality rate. Genomic analysis has identified a lineage with limited internal diversity most closely related to a genome sequence from a sporadic case sampled in 2014 in Uganda, though the lineages have diverged from a common ancestor that was circulating for decades in the animal reservoir.

Notably, the data also provide evidence that the outbreak resulted from a single zoonotic transmission event with limited human-to-human transmission, rather than multiple independent zoonotic transmission events. The Rwandan MVD outbreak prompted a thorough investigation that included contact tracing, clinical assessment, travel history, sequencing, and serology testing, to trace the virus's origin. Results of investigations linked the index case to a mining cave inhabited by *Rousettus aegyptiacus* (the Egyptian fruit bat), where three individuals tested seropositive for IgG and IgM, further supporting the zoonotic origin of the outbreak through human-animal interactions.

***Background***

Since its discovery in 1967, the Marburg virus disease (MVD) has emerged as a significant global health threat, resulting in several outbreaks characterized by alarmingly high case fatality rates ranging from 22% to 90% (1). The first reported instances of MVD occurred in simultaneous outbreaks in Marburg and Frankfurt, Germany, as well as in Belgrade, Yugoslavia (now Serbia) (2). To date, there have been 19 recorded outbreaks, 563 confirmed cases, and 428 deaths worldwide (4). On September 27, 2024, Rwanda reported its first ever cases of MVD (5). The

91 ongoing outbreak in Rwanda has confirmed 66 cases, with a case fatality rate of approximately
92 23% (5).
93
94 MVD has two distinct variants: Marburg virus (MARV) and Ravn virus (RAVV), with MARV
95 being the more prevalent variant, responsible for the majority of sporadic MVD outbreaks
96 worldwide. MARV is a negative-sense single-stranded RNA virus from the Filoviridae family,
97 similar to Ebola and possesses inverse-complementary 3′ and 5′ termini (3). MVD is
98 predominantly a zoonosis, transmitting to humans from either the bat natural reservoir or through
99 intermediate hosts, including non-human primates. The mechanisms by which bats regulate viral
100 replication and maintain complex immunity in contrast to humans remain unclear due to a lack of
101 bat-specific research tools necessary for comparative studies, such as antibodies for flow
102 cytometry, genomics, and transcriptomics (1,2). Studies confirm that MARV's natural reservoir
103 is the Egyptian fruit bat (*Rousettus aegyptiacus*) (6). The virus can cause viral hemorrhagic fever
104 in both humans and primates. However, the precise transmission dynamics between the natural
105 reservoir and humans or primates are insufficiently understood, though exposure to contaminated
106 excretions from fruit bats is likely a contributing factor (6). The virus is transmitted from human
107 to human, particularly through direct contact with body fluids like blood, saliva, semen, and other
108 body fluids from infected individuals (7).
109
110 The Marburg viral genome consists of 19,114 nucleotides encoding for seven proteins, including
111 glycoprotein (GP), nucleoprotein (NP) virion protein 30 (VP30), VP35, VP24, VP40 and large
112 viral polymerase (3).
113

114 Genomic characterization of MARV strains has revealed substantial genetic diversity across its
115 global phylogeny, but exhibits limited genomic variation within outbreaks (8).
116 Sequencing of the Marburg genome has provided deeper insights into viral evolution and identified
117 critical mutation hotspots during adaptation to new hosts, particularly in the VP40 protein and the
118 NP-VP35 intergenic region (9). These mutations can influence the virus's ability to evade the
119 immune system, therefore enhancing its pathogenicity.
120
121 ***Statement of the specific scope of the study***
122 In this study, we used a near real-time genomics sequencing approach to characterize the Marburg
123 virus in blood samples obtained from patients in the ongoing outbreak in Rwanda. Our aim was to
124 use the genomic sequencing data to identify and characterize the virus and understand its evolution
125 and transmission dynamics during the current outbreak. This research underscores the importance
126 of continuous genomic surveillance which not only facilitates outbreak tracking but also informs
127 public health strategies for effectively controlling this deadly pathogen.
128
129 ***Results***
130
131 Phylogenetic analyses support that the outbreak resulted from a single zoonotic transmission event
132 with limited human-to-human transmission rather than multiple independent zoonotic
133 transmission events (**Figure 1A**). Multiple independent zoonotic transmissions would have
134 resulted in a set of more diverged sequences introduced from the genetically diverse viral
135 population in the reservoir (10). The probable index case was a man in his 20's with an
136 occupational exposure to fruit bats (*Rousettus aegyptiacus*) in a mining cave environment, who

137 exhibited symptoms highly consisting with the classic clinical presentation of MVD. Additionally,
138 serological testing of three contacts of the index case exhibited MARV antibodies, further
139 supporting epidemiological tracing of the index case. The outbreak lineage is most closely related
140 to a sequence sampled in Kampala, Uganda in September 2014 from a healthcare worker (HCW),
141 with no secondary cases observed (KP985768). The source of the zoonotic transmission in 2014
142 was never identified (11). However, the Rwanda-Uganda sister lineages are significantly diverged
143 from one another, separated by 82 nucleotide substitutions (**Figure 1A**). In Bayesian phylogenetic
144 reconstructions, we estimate that the two lineages diverged from a common ancestor that circulated
145 in the animal reservoir in November 2008 [95% highest posterior density, or HPD: May 2007 and
146 June 2010] (**Supplementary Figure 1 A-B**).
147
148 The outbreak lineage in Rwanda is nested within a larger clade that includes diversity sampled
149 from bats in southwestern Uganda from 2007 onwards, along with two human cases identified in
150 Uganda in 2017 (**Figure 1A, B**). The closest bat virus (JX458855) was sampled from a juvenile
151 Egyptian fruit bat (*Rousettus Aegyptiacus)* in 2009 from Python Cave in Queen Elizabeth National
152 Park, a popular tourist attraction in south western Uganda (**Figure 1B**) (6). The lineage in Rwanda
153 is significantly diverged from JX458855, sharing a common ancestor that likely circulated in the
154 reservoir as early as June 2006 (95% HPD: December 2004 to November 2007) (**Supplementary**
155 **Figure 1 A-B**). *Rousettus aegyptiacus* are a cave dwelling species, with spillover events and
156 limited outbreaks frequently associated with mining activities. This includes outbreaks and
157 sporadic cases linked to Python cave and the Kitaka mine that is only 50 km away in 2007 and
158 2008, which both hosts *Rousettus aegyptiacus* colonies of over 50 000 bats. (6,10,12). The
159 divergent relationship of the Rwandan Marburg virus outbreak lineage indicates that the virus's

dispersal through host networks involved larger scale animal movement over a long period of time, rather than a direct ancestral connection to the *Rousettus aegyptiacus* colony in southwestern Uganda.

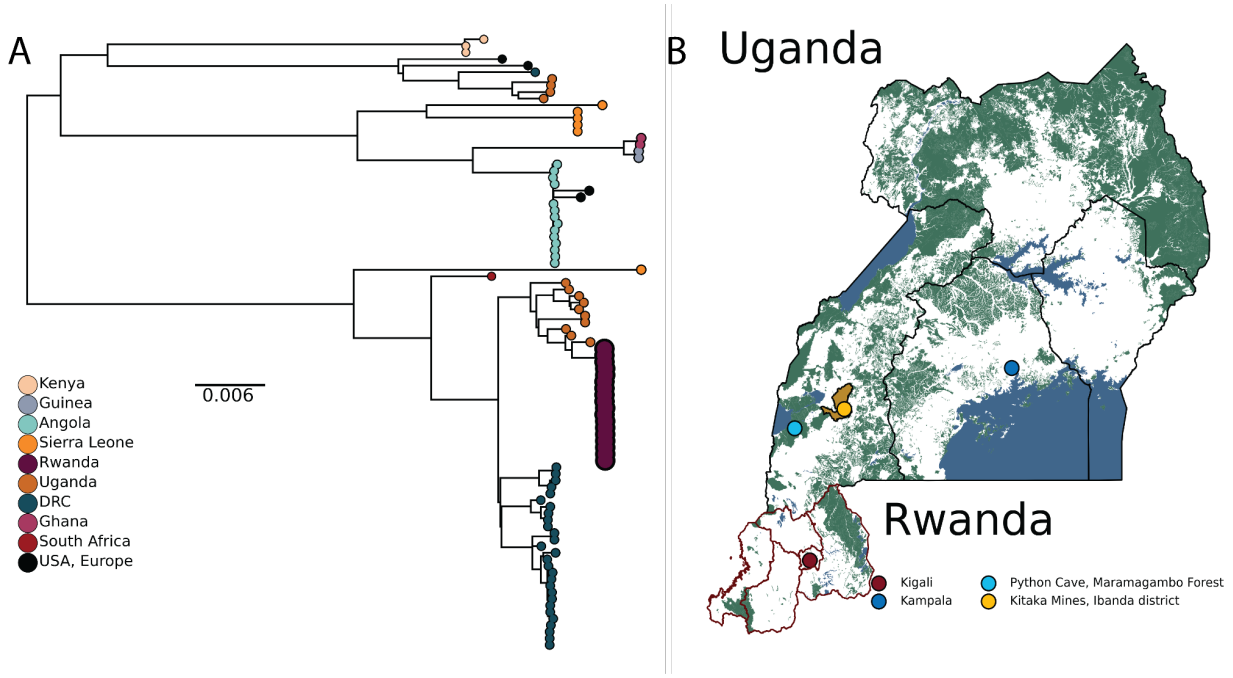


**Figure 1**: *A) Maximum likelihood phylogeny of the global MARV dataset. Tips are annotated by country of isolation. This study's tips are relatively enlarged. B) Map of Uganda and Rwanda. The city of patients in this study (Kigali) is annotated in dark red. Python Cave and Kitaka Mine in Ibanda district in southwestern Uganda are annotated in light blue and yellow, respectively.*

The index patient's close relative was admitted to Hospital 1 (H1) at the end of August 2024 but succumbed to the illness prior to the definitive diagnosis of MVD. It is highly probable that this patient infected healthcare workers (HCWs) at H1, where MVD was subsequently confirmed at the end of September 2024. From 22-28 September, 26 cases were reported in HCWs at H1 and H2, respectively. The limited genetic variation among the outbreak sequences was consistent with

175 a very recent common ancestor, the short sampling period, and previous observations from the
176 Angola MARV outbreak (**Figure 2A**) (12). A cluster of eight identical sequences was sampled,
177 spanning the full sampling period (C1 in **Figure 2A, B**). The majority of the C1 sequences were
178 isolated from healthcare workers (HCWs) at H1 from 22-28 September, with reported symptom
179 onset as early as mid-September (**Figure 2B**). A C1 sequence was sampled from a HCW at H2 at
180 the end of September, suggesting infection from an unsampled C1 case in H2 or dissemination
181 between the two healthcare facilities. There are recorded cases of healthcare workers moving
182 between healthcare settings H1 and H2. This is further supported by cluster C2, consisting of two
183 healthcare workers from H1 and H2 respectively that share the synonymous SNP C11070T relative
184 to C1. Both C2 cases report symptom onset and were sampled in the later weeks of the epidemic.
185 There are a further seven identical sequences (C4) sampled between H1 and H2 across the full
186 sampling period that are one synonymous SNP (T10031C) away from C1. C002, a healthcare
187 worker employed at both H1 and H2, is believed to have acquired the infection at H1. This
188 individual subsequently became the index case at H2, leading to a nosocomial cluster at H2 and
189 infections at H1. Overall, there were only three synonymous SNPs observed in the outbreak clade:
190 A5856G (n=1 sequence), T10031C (n=7), and C11070T (n=2). A5856G and T10031C as well as
191 C11070T are outside of the CDS of the GP and VP24 genes, respectively. There is therefore no
192 evidence that post-emergence substitutions enhanced human transmission.

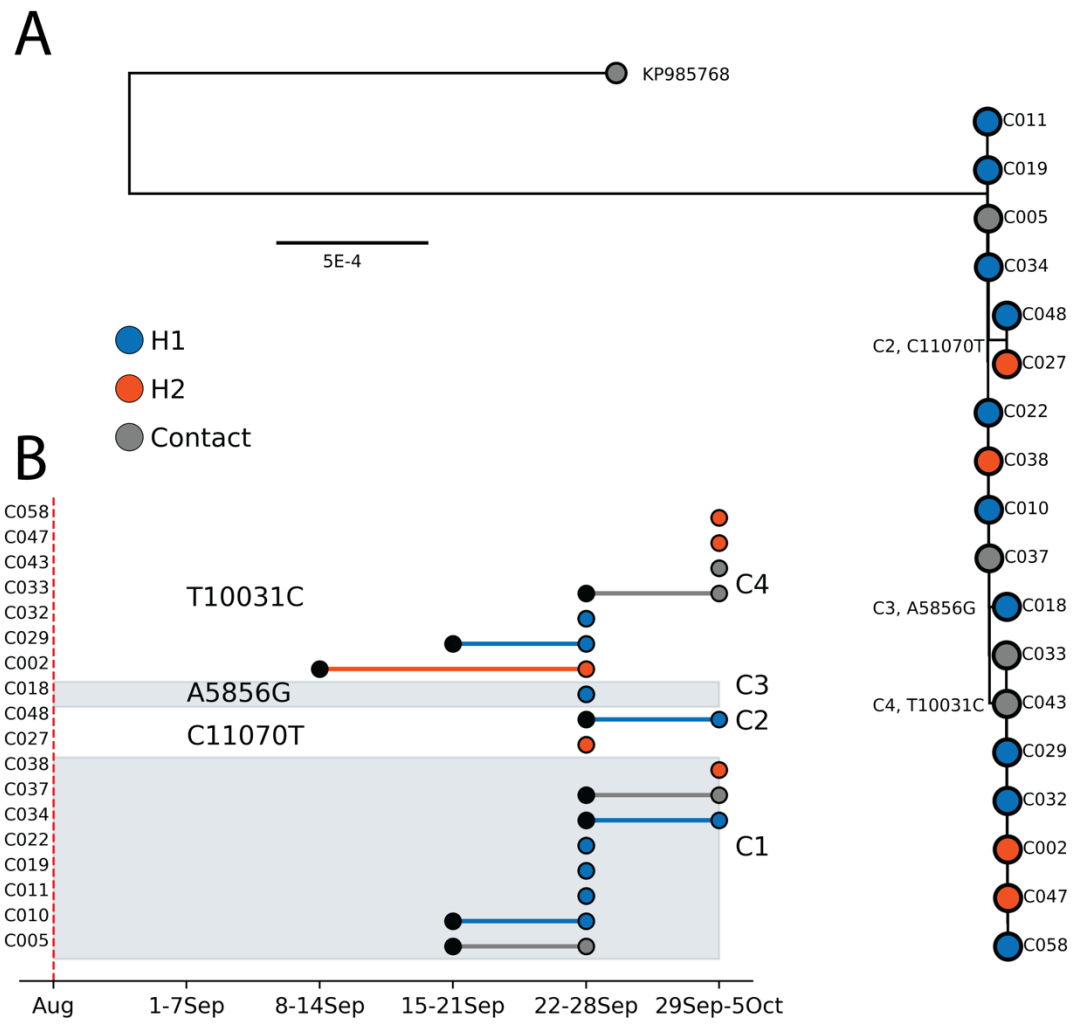


**Figure 2**: *A) Maximum likelihood phylogeny of the outbreak clade, with the Kampala outgroup. Sequences are colored with associated hospital. SNPs reconstructed relative to the common ancestor are annotated in text, as are the clusters defined by the SNP presence. The coordinates are relative to NC_001608 B) Epidemiological timeline of the sampled sequences in Figure 2A, as annotated on the y-axis. The first black marker, if present, indicates the week of symptom onset if distinct from week of sampling, with the second indicating the week of sampling. Sequences are colored by their associated hospital (H1, H2), and partitioned by SNP presence into clusters, as annotated in text. Red dashed line indicates the contact of the index case admitted to H1.*

203 An exhaustive investigation of all cases was conducted which led to identifying the index case.
204 This in-depth process involved a comprehensive collection of diverse data sources including
205 clinical records, travel history, antibody serology testing results, and contact tracing information.
206 This evidence revealed that the earliest patient was traced back to a mining cave and exhibited
207 symptoms highly consisting with the classic clinical presentation of MVD. Additionally, serology
208 testing results from three contacts linked to the index case exhibited antibodies of persons exposed
209 to Marburg virus. This suggests that the mining cave may have served as a potential habitat for the
210 MARV animal reservoir, particularly the fruit bat (*Rousettus aegyptiacus*). Following up on these
211 findings, the Rwanda Ministry of Health through a multisectoral collaboration launched an
212 investigation surveillance with the aim of screening fruit bats, mainly cave dwellers, for Marburg
213 virus (**Supplementary Figures 2 A, B and C**).
214

215 ***Discussion***

216 The Rwanda MVD outbreak exhibited substantial human-to-human transmission, primarily
217 involving healthcare personnel, as is often observed with viral hemorrhagic fever (VHF) outbreaks
218 closely associated with nosocomial and occupational infections (18). However, Rwanda
219 effectively contained the spread from further reaching the broader community. Positive cases were
220 promptly isolated and treated with monoclonal antibodies and antivirals, achieving a favorable
221 case fatality rate of approximately 23%. This underscores the ongoing need to enhance healthcare
222 personnel's knowledge and attitudes regarding VHF case management.
223 Through evolutionary and phylogenetic analysis, we observed that the early outbreak sequences
224 represented very limited genomic variation, indicating that the outbreak originated from a single
225 zoonotic transmission event. The Rwandan lineage shared a common ancestor with sequences

originating from diversity sampled in bats in southwestern Uganda, thought the lineages had diverged over decades in the animal reservoir. It is likely that enhanced zoonotic surveillance will reveal many unsampled intermediates that can clarify the ecological pathways of transmission between bat colonies in Uganda and Rwanda. Previous research indicates that bats can harbor MARV for extended periods, with active mining areas in Rwanda providing ideal habitats for bats and increasing the likelihood of zoonotic transmission (19).

We observed three synonymous single nucleotide polymorphisms (SNPs) outside the coding regions of the GP and VP24 genes, respectively. Studies have shown that the Marburg virus VP24 protein interacts with the nucleoprotein (NP) and other cellular membranes, facilitating the release of new virions from infected cells (20). Additionally, research highlights that MARV VP24 directly interacts with the human and bat Keap1 proteins, which modulate antioxidant responses to support viral replication, a strategy likely critical for viral persistence and host adaptation (21). Genomic sequencing of MARV in Rwanda has yielded critical insights into viral circulation dynamics. However, as these SNPs fall outside of coding regions, it is unlikely that they functionally contribute to enhanced viral fitness on any scale. Our results should be interpreted within the context of our smaller sample size, which only covers the first two weeks of the outbreak.

This research underscores the importance of continuous genomic surveillance which not only facilitates outbreak tracking but also informs public health strategies for effectively controlling this deadly pathogen. In addition, previous research indicates that bats can harbor MARV for extended periods, with active mining areas in Rwanda providing ideal habitats for bats and

249 increasing the likelihood of zoonotic transmission. Furthermore, Rwanda's location in a region of
250 consistent turbulent outbreaks, including Ebola, Rift Valley fever, COVID-19, dengue, and
251 Marburg, underscores the importance of regional and international collaboration to enhance
252 outbreak preparedness and responses for global health security.
253
254

255 **Reference**

256 1. Mehedi M, Groseth A, Feldmann H, Ebihara H. Clinical Aspects of Marburg
257 Hemorrhagic Fever. Future Virol [Internet]. 2011 Sep [cited 2024 Oct 24];6(9):1091–106.
258 Available from: https://www.tandfonline.com/doi/full/10.2217/fvl.11.79
259

260 2. Kilangisa LM, Max BL, Kayuni EA, Shao ER, Mashauri HL. Marburg virus disease:
261 lesson learned from the first outbreak encounter in Tanzania. International Journal of Surgery:
262 Global Health [Internet]. 2023 Jul [cited 2024 Oct 17];6(4). Available from:
263 https://journals.lww.com/10.1097/GH9.0000000000000186
264

265 3. Paton, A. W., & Paton, J. C. (2018). Detection and characterization of Shiga toxigenic
266 *Escherichia coli* by PCR. In D. Liu (Ed.), Molecular Medical Microbiology (2nd ed., pp. 213–
267 239). Academic Press. https://doi.org/10.1016/B978-0-12-812026-2.00013-X
268

269 4. Srivastava S, Sharma D, Kumar S, Sharma A, Rijal R, Asija A, et al. Emergence of Marburg
270 virus: a global perspective on fatal outbreaks and clinical challenges. Front Microbiol [Internet].
271 2023 Sep 13 [cited 2024 Oct 14];14:1239079. Available from:
272 https://www.frontiersin.org/articles/10.3389/fmicb.2023.1239079/full
273 5. Ministry of health R. Stop the Marburg virus [Internet]. 2024 Oct. Available from:
274 https://x.com/rwandahealth/status/1846968616278778288?s=12&t=HFAKR78RPRo-
275 Cmz7j7ciDQ
276
277

6. Amman BR, Carroll SA, Reed ZD, Sealy TK, Balinandi S, Swanepoel R, et al. Seasonal Pulses of Marburg Virus Circulation in Juvenile Rousettus aegyptiacus Bats Coincide with Periods of Increased Risk of Human Infection. Kawaoka Y, editor. PLoS Pathog [Internet]. 2012 Oct 4 [cited 2024 Oct 18];8(10):e1002877. Available from: https://dx.plos.org/10.1371/journal.ppat.1002877

7. Amman BR, Schuh AJ, Albariño CG, Towner JS. Marburg Virus Persistence on Fruit as a Plausible Route of Bat to Primate Filovirus Transmission. Viruses [Internet]. 2021 Nov 30 [cited 2024 Oct 18];13(12):2394. Available from: https://www.mdpi.com/1999-4915/13/12/2394

8. Towner JS, Khristova ML, Sealy TK, Vincent MJ, Erickson BR, Bawiec DA, et al. Marburgvirus Genomics and Association with a Large Hemorrhagic Fever Outbreak in Angola. J Virol [Internet]. 2006 Jul [cited 2024 Oct 19];80(13):6497–516. Available from: https://journals.asm.org/doi/10.1128/JVI.00069-06

9. Wei H, Audet J, Wong G, He S, Huang X, Cutts T, et al. Deep-sequencing of Marburg virus genome during sequential mouse passaging and cell-culture adaptation reveals extensive changes over time. Sci Rep [Internet]. 2017 Jun 13 [cited 2024 Oct 19];7(1):3390. Available from: https://www.nature.com/articles/s41598-017-03318-3

10. Towner JS, Amman BR, Sealy TK, Carroll SAR, Comer JA, Kemp A, et al. Isolation of Genetically Diverse Marburg Viruses from Egyptian Fruit Bats. Fouchier RAM, editor. PLoS

Pathog [Internet]. 2009 Jul 31 [cited 2024 Oct 25];5(7):e1000536. Available from: https://dx.plos.org/10.1371/journal.ppat.1000536

11. Nyakarahuka L, Ojwang J, Tumusiime A, Balinandi S, Whitmer S, Kyazze S, Kasozi S, Wetaka M, Makumbi I, Dahlke M, Borchert J, Lutwama J, Ströher U, Rollin PE, Nichol ST, Shoemaker TR. Isolated Case of Marburg Virus Disease, Kampala, Uganda, 2014. Emerg Infect Dis. 2017 Jun;23(6):1001-1004. doi: 10.3201/eid2306.170047. PMID: 28518032; PMCID: PMC5443453

12. Carroll SA, Towner JS, Sealy TK, McMullan LK, Khristova ML, Burt FJ, et al. Molecular Evolution of Viruses of the Family Filoviridae Based on 97 Whole-Genome Sequences. J Virol [Internet]. 2013 Mar [cited 2024 Oct 25];87(5):2608–16. Available from: https://journals.asm.org/doi/10.1128/JVI.03118-12

13. Chen S. Ultrafast one-pass FASTQ data preprocessing, quality control, and deduplication using fastp. iMeta [Internet]. 2023 May [cited 2024 Oct 24];2(2):e107. Available from: https://onlinelibrary.wiley.com/doi/10.1002/imt2.107

14. Langmead B, Salzberg SL. Fast gapped-read alignment with Bowtie 2. Nat Methods [Internet]. 2012 Apr [cited 2024 Oct 25];9(4):357–9. Available from: https://www.nature.com/articles/nmeth.1923

322 15. Li H. Minimap2: pairwise alignment for nucleotide sequences. Birol I, editor.
323 Bioinformatics [Internet]. 2018 Sep 15 [cited 2024 Oct 25];34(18):3094–100. Available from:
324 https://academic.oup.com/bioinformatics/article/34/18/3094/4994778
325
326 16. Grubaugh ND, Gangavarapu K, Quick J, Matteson NL, De Jesus JG, Main BJ, et al. An
327 amplicon-based sequencing framework for accurately measuring intrahost virus diversity using
328 PrimalSeq and iVar. Genome Biol [Internet]. 2019 Dec [cited 2024 Oct 25];20(1):8. Available
329 from: https://genomebiology.biomedcentral.com/articles/10.1186/s13059-018-1618-7
330
331 17. Wilm A, Aw PPK, Bertrand D, Yeo GHT, Ong SH, Wong CH, et al. LoFreq: a sequence-
332 quality aware, ultra-sensitive variant caller for uncovering cell-population heterogeneity from
333 high-throughput sequencing datasets. Nucleic Acids Research [Internet]. 2012 Dec 1 [cited 2024
334 Oct 25];40(22):11189–201. Available from:
335 https://academic.oup.com/nar/article/40/22/11189/1152727
336
337 18. Raab, M., Pfadenhauer, L.M., Millimouno, T.J. et al. Knowledge, attitudes and practices
338 towards viral haemorrhagic fevers amongst healthcare workers in urban and rural public healthcare
339 facilities in the N'zérékoré prefecture, Guinea: a cross-sectional study. BMC Public Health 20,
340 296 (2020). https://doi.org/10.1186/s12889-020-8433-2
341
342 19. Scarpa F, Bazzani L, Giovanetti M, Ciccozzi A, Benedetti F, Zella D, Sanna D, Casu M,
343 Borsetti A, Cella E, et al. Update on the Phylodynamic and Genetic Variability of Marburg Virus.
344 Viruses. 2023; 15(8):1721. https://doi.org/10.3390/v15081721

20. Abir, M. H., Rahman, T., Das, A., Etu, S. N., Nafiz, I. H., Rakib, A., … Hassan, M. M. (2022). Pathogenicity and virulence of Marburg virus. Virulence, 13(1), 609–633. https://doi.org/10.1080/21505594.2022.2054760

21. Edwards MR, Johnson B, Mire CE, Xu W, Shabman RS, Speller LN, Leung DW, Geisbert TW, Amarasinghe GK, Basler CF. The Marburg virus VP24 protein interacts with Keap1 to activate the cytoprotective antioxidant response pathway. Cell Rep. 2014 Mar 27;6(6):1017-1025. doi: 10.1016/j.celrep.2014.01.043. Epub 2014 Mar 13. PMID: 24630991; PMCID: PMC3985291.

22. Kazutaka Katoh, Daron M. Standley, MAFFT Multiple Sequence Alignment Software Version 7: Improvements in Performance and Usability, Molecular Biology and Evolution, Volume 30, Issue 4, April 2013, Pages 772–780, https://doi.org/10.1093/molbev/mst010

23. Bui Quang Minh, Heiko A Schmidt, Olga Chernomor, Dominik Schrempf, Michael D Woodhams, Arndt von Haeseler, Robert Lanfear, IQ-TREE 2: New Models and Efficient Methods for Phylogenetic Inference in the Genomic Era, Molecular Biology and Evolution, Volume 37, Issue 5, May 2020, Pages 1530–1534, https://doi.org/10.1093/molbev/msaa015.

24. Kalyaanamoorthy, S., Minh, B., Wong, T. *et al.* ModelFinder: fast model selection for accurate phylogenetic estimates. Nat. Methods 14, 587–589 (2017). https://doi.org/10.1038/nmeth.4285.

25. Diep Thi Hoang, Olga Chernomor, Arndt von Haeseler, Bui Quang Minh, Le Sy Vinh, UFBoot2: Improving the Ultrafast Bootstrap Approximation, Molecular Biology and Evolution, Volume 35, Issue 2, February 2018, Pages 518–522, https://doi.org/10.1093/molbev/msx281.

26. Pavel Sagulenko, Vadim Puller, Richard A Neher, TreeTime: Maximum-likelihood phylodynamic analysis, Virus Evolution, Volume 4, Issue 1, January 2018, vex042, https://doi.org/10.1093/ve/vex042.

27. Carroll SA, Towner JS, Sealy TK, McMullan LK, Khristova ML, Burt FJ, Swanepoel R, Rollin PE, Nichol ST. Molecular evolution of viruses of the family Filoviridae based on 97 whole-genome sequences. J Virol. 2013;87:2608–2616. doi: 10.1128/JVI.03118-12.

28. Bouckaert, R., Heled, J., Kühnert, D., Vaughan, T., Wu, C-H., Xie, D., Suchard, MA., Rambaut, A., & Drummond, A. J. (2014). BEAST 2: A Software Platform for Bayesian Evolutionary Analysis. PLoS Computational Biology, 10(4), e1003537. doi:10.1371/journal.pcbi.1003537.

**Acknowledgments**

We gratefully acknowledge the support of the Government of Rwanda and the Ministry of Health, through the Rwanda Biomedical Center, for facilitating and supporting this sequencing work. We extend our sincere appreciation to both the African Centre of Excellence for Genomics of Infectious Diseases (ACEGID) and the Africa Centre for Disease Control and Prevention (Africa

CDC) for their invaluable contributions. This work was made possible through the collaborative efforts of development partners and stakeholders, to whom we are deeply grateful.

**Funding:** Government of Rwanda and Development Partners.

**Author contributions**

Conceptualization: Y.B, L.M, S.N, C.H, C.M.M, Methodology: Y.B, L.M, A.A, E.U, R.M, E.P, P.S, C.H, C.M.M Investigation: I.M, E.R, E.K, E.R, N.G Sampling: R.S, P.G, P.S, J.C.M PCR Experiment: E.K, F.U, V.M, G.I, H.M Sequencing: Y.B, L.M, E.U, L.I, C.M, A.U, I.U, R.N, A.U, J.K, J.P.M Bioinformatics Analysis: E.P, R.M, J.P.M, N.G, J.R, A.O, C.H Lab Enablement: S.T.K, A.A, O.O, O.A, A.H, C.M.M Writing- Original Draft: Y.B, L.M, C.M, R.M, J.P.M, P.S Writing Review and Editing: Y.B, L.M, E.E.S.F, E.R, C.M, M.S, M.N, T.T, D.T, E.S, M.G, J.P.R, J.N, A.R, F.K, G.M, A.A, S.N, C.H, C.M.M.

**Diversity, equity, ethics, and inclusion [optional]:** NA

**Competing interests:** The authors declare no conflicts of interest.

**Data and code availability**

All the sequence data are available upon request on https://github.com/rbx-bfx/illumina_vsp**.**

***Materials and Methods***

**Ethics declaration**

412 The study was approved by the Rwanda National Ethics Committee (FWA Assurance No.
413 00001973 IRB 00001497 of IORG0001100-Protocol approval notice: N° 121/RNEC/2024).
414
415 **Patient sample collection**
416 We obtained whole blood samples from suspected patients presented with clinical symptoms (high
417 fever, severe headaches, muscle aches, fatigue, nausea, vomiting, and diarrhea) of MDV. Sample
418 testing was performed at Rwanda Biomedical Centre/National Reference Laboratory whereby
419 samples were kept in a cold chain prior to plasma separation and analysis.
420
421 **Nucleic acid extraction**
422 Viral RNA was extracted from 140µl plasma using the QIAamp Viral RNA Mini Kit (Qiagen,
423 Hilden, Germany), following the manufacturer's instructions adapted to the in-house standard
424 operating procedures with an elution volume of 60µl. The extracted RNA was quantified using a
425 Qubit fluorometer, and the samples were stored at -80°C until further analysis.
426
427 **RT-PCR and genomic sequencing**
428 For the detection and amplification of the target regions of the MVD, we employed the use of
429 RealStar® Filovirus Screen RT-PCR Kit 1.0 (Altona Diagnostics, Hamburg, Germany), which is
430 based on real-time PCR technology, for the qualitative detection and differentiation of Ebola and
431 Marburg virus specific RNA in human EDTA plasma. The RT-qPCR was conducted following
432 manufacturer's user guide and performed on CFX96 BIORAD machine. The amplification
433 followed an initial denaturation at 95°C for 5 minutes, followed by 40 cycles of denaturation at
434 95°C for 30 seconds, annealing at 55°C for 30 seconds, and extension at 72°C for 1 minute,

435 concluding with a final extension at 72°C for 5 minutes. The amplified products were analyzed via
436 2% agarose gel electrophoresis to confirm successful amplification and appropriate product size.
437 Following amplification, library construction was performed on 30 samples using the Illumina
438 RNA Prep with Enrichment (L) Tagmentation (IRPE) workflow and the lllumina Viral
439 Surveillance Panel v2 kit (VSP v2 kit). Total RNA extracts were converted to cDNA, tagmented
440 and thereafter amplified. Genomic region of interest was captured using a hybrid capture method.
441 Probes were isolated using magnetic pulldown which are selectively enriched for the desired
442 regions. Enriched libraries were quantified using dsDNA HS assay and Qubit fluorometer.
443 Libraries were thereafter denatured and normalized at a final loading concentration of 0.8pM.
444 Paired-end sequencing was performed using a NextSeq 550 with a 300-cycle mid-output cartridge,
445 with the sequencing depth aimed at a minimum coverage of 100x to ensure robust variant
446 detection.
447
448 **Bioinformatics Analysis**
449 **Genome Assembly**
450 We employed a reference-based genome assembly pipeline to analyze the sequencing data
451 generated using the Illumina Viral Surveillance Panel (VSP) v2 Kit (described above). This
452 workflow integrates several steps including; quality control, host genome filtering, and viral
453 genome assembly to accurately reconstruct viral sequences from targeted sequencing.
454 To ensure that only high-quality data were processed downstream, raw sequencing reads were first
455 processed with *fastp v. 0.23.24 (13)* for trimming adapters and filtering out low-quality bases.
456 Following this, human host genome sequences were filtered out by aligning the cleaned reads to
457 the human genome (hg38) using *Bowtie2 v.2.5.4* (14). Unmapped reads, presumed to be of viral

458 origin, were retained for downstream analysis. These de-hosted reads were then aligned to a
459 Marburg virus reference genome (NC_001608.3) using *Minimap2 v.2.28 (15)*,
460 The sequences had 70-97% genomic coverage. We manually masked two mutations in respective
461 consensus sequences that were adjacent to potential misalignment.
462

463 **Variant Calling and Consensus Generation**

464 Variant calling was performed using both *ivar 1.4.3 (16)* and *LoFreq v.2.1.5 (17)*. A depth
465 coverage threshold of 50 reads per nucleotide position was applied to ensure robust and reliable
466 variant detection. This threshold was also applied to the generation of consensus sequences which
467 was also done using *ivar 1.4.3*.,
468

469 **Phylogenetic**

470 We combined our eighteen higher quality sequences (coverage >= 70%) with all publicly available
471 MARV sequences available on Genbank (N=81). To root the tree, we included 8 Ravn virus
472 sequences included as an outgroup, which were pruned from the tree and excluded in all
473 subsequent analyses. We aligned the sequences using *Mafft v 7.52 (22)* and reconstructed a
474 phylogenetic tree using *IQTree 2.2.5 (23)* under modelfinder plus *(24)*, with ultrafast bootstrapping
475 (25). We performed the initial ancestral state reconstruction using *Treetime v0.9.3 (26)*.
476

477 **Bayesian phylogenetic reconstruction**

478 The current genomic data does not provide sufficient temporal signal to estimate the rate of
479 evolution in the outbreak clade. However, we were not interested in estimating the time to the most
480 recent common ancestor (tMRCA) of the outbreak clade, as determining the emergence timing of

481 the outbreak clade will more likely depend on the epidemiological and contact history of the index
482 case. We wanted to estimate tMRCA of the outbreak clade and its closest human and zoonotic
483 outgroups to better understand its potential zoonotic emergence pathway. We therefore
484 reconstructed the time-resolved phylogeny under a fixed local clock. We assumed a fixed value of
485 1e-3 substitutions per site per year as a plausible rate of evolution for a RNA virus in the early
486 stage of an outbreak for the defined outbreak clade. We allowed the remainder of the tree to evolve
487 under a lognormal prior centered on 5e-4. (27) We used a two-phase coalescent model: the tree
488 from the MRCA (Rwandan lineage) onward was modeled with an exponential growth model, with
489 the earlier phase modeled as a constant-population size coalescent model. We ran two independent
490 chains of 100 million states to ensure convergence, discarding the initial 10% of each chain as
491 burn-in. The chains were then combined with LogCombiner. For all subsequent analyses, we
492 assessed convergence using Tracer, and constructed a maximum clade credibility (MCC) tree in
493 TreeAnnotator 1.10 (28).
494
495
496
497
498
499
500
501
502
503
504

505 **Supplemental Figures**

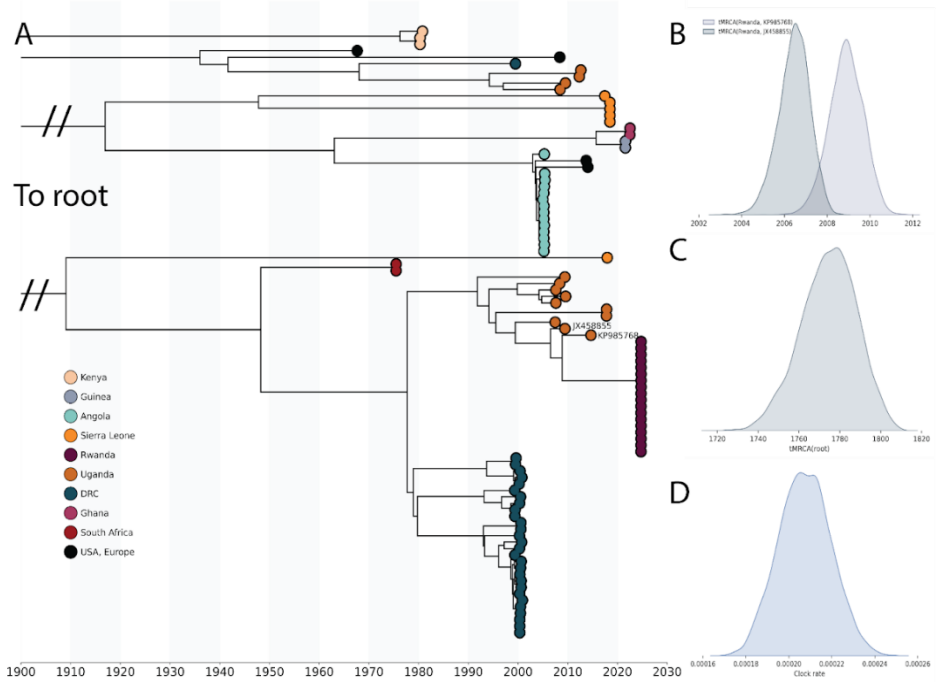


506

507

508 **Supplemental Figure 1:** *A) Time resolved maximum clade credibility tree of global MARV*
509 *dataset, with closest human (KP985768) and zoonotic (JX458855) sequence to the Rwandan*
510 *outbreak lineage annotated. B) tMRCA of the Rwandan lineage and KP985768 as well as*
511 *JX458855 respectively. C) tMRCA of root, which is truncated in A for clarity. D) Estimate clock*
512 *rate in substitutions per site per year for full tree, excluding the outbreak clade.*

513

514

515

**Supplemental Figure 2:** *A) Mining cave entrance with human activity; B) Trapping fruit bats with net; C) Sampling bats for Marburg virus.*

# Figures

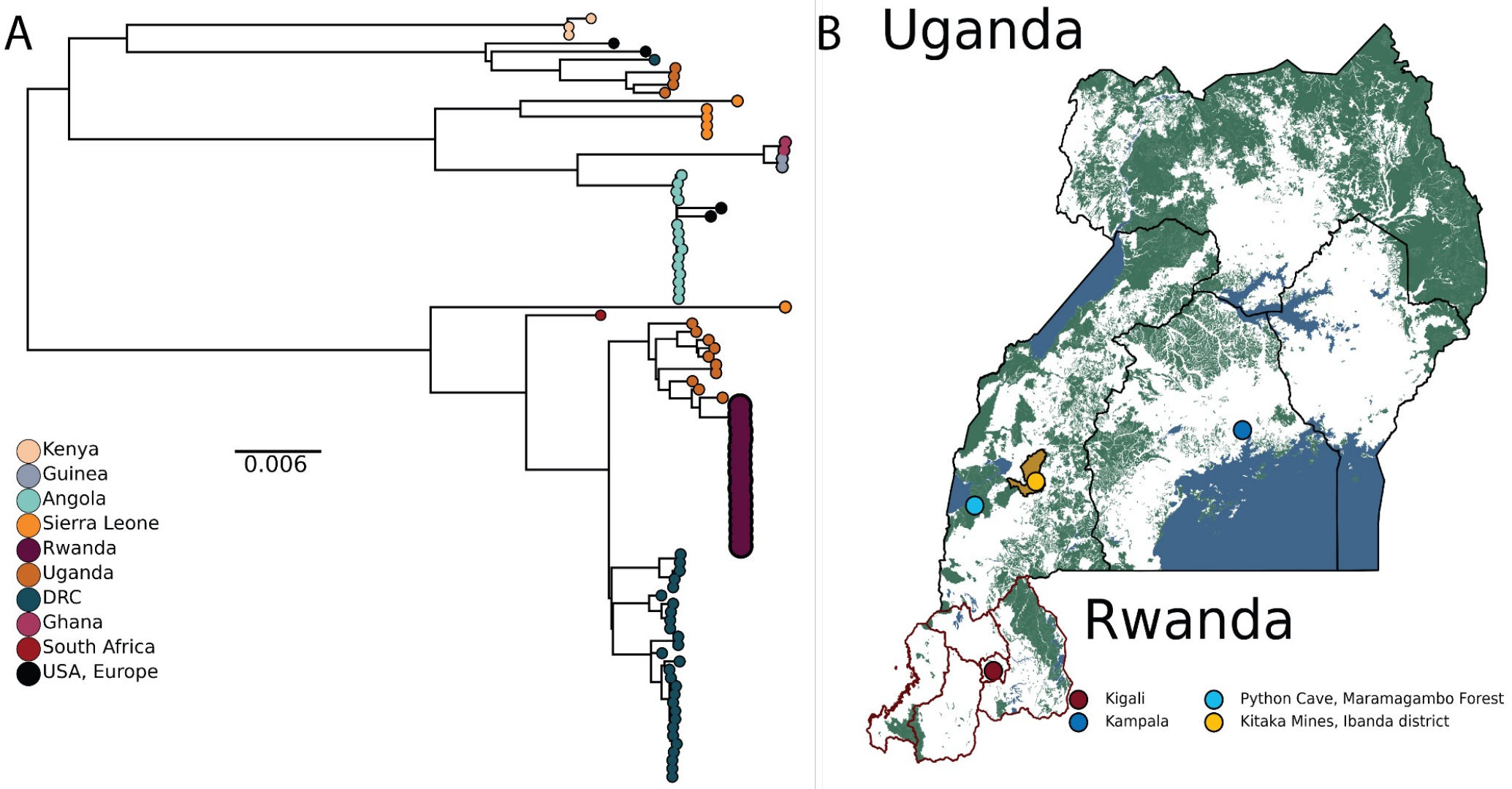


**Figure 1:** *A) Maximum likelihood phylogeny of the global MARV dataset. Tips are annotated by country of isolation. This study's tips are relatively enlarged. B) Map of Uganda and Rwanda. The city of patients in this study (Kigali) is annotated in red. Python Cave and Kitaka Mine in Ibanda district in southwest Uganda are annotated in light blue and yellow, respectively.*

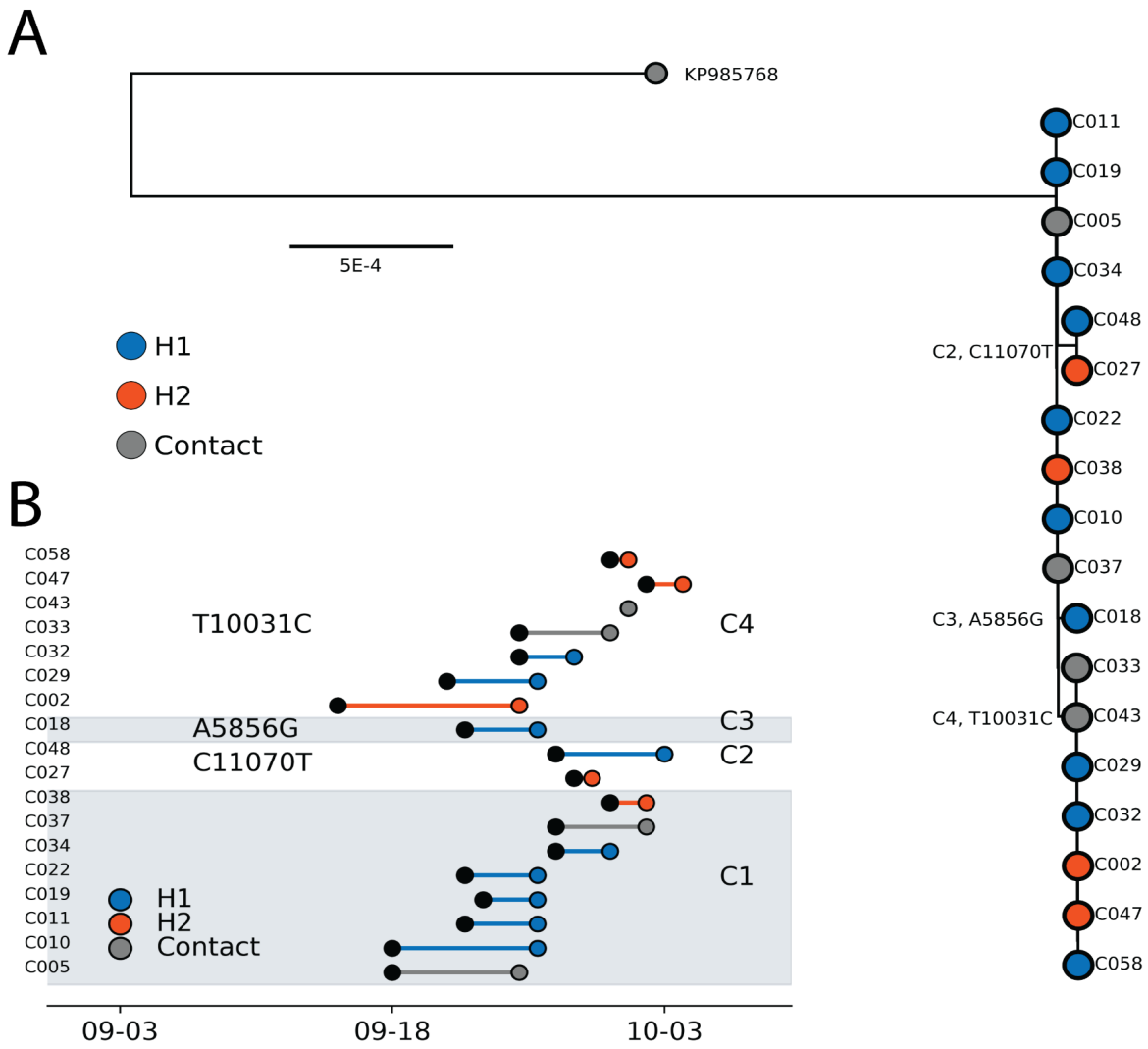


**Figure 2:** *A) Maximum likelihood phylogeny of the outbreak clade, with the Kampala outgroup. Sequences are colored with associated hospital. SNPs reconstructed relative to the common ancestor are annotated in text, as are the clusters defined by the SNP presence. The coordinates are relative to NC_001608 B) Epidemiological timeline of the sampled sequences in Figure 2A, as annotated on the y-axis. The first black marker indicates the date of symptom onset, with the second indicating the date of sampling. Sequences are colored by their associated hospital (H1, H2), and partitioned by SNP presence into clusters, as annotated in text*